

NOVEL TETRAZOLE AND 1,3,4-OXADIAZOLE DERIVATIVES SYNTHESIS, MOLECULAR DOCKING, ADME, POTENTIAL ACTIVATOR FOR RABBIT MUSCLE PYRUVATE KINASE

Mustafa Oğuzhan KAYA^{a,*}, Tuna DEMİRCİ^b, Selman KARİPÇİN^c,
Oğuzhan ÖZDEMİR^d, Yeşim KAYA^a, Mustafa ARSLAN^c

ABSTRACT. The activation of muscle pyruvate kinase (PK) increases the conversion of phosphoenolpyruvate (PEP) to pyruvate, which results in the production of ATP. This is critical for supplying the energy needed for muscle contraction. In this study, we synthesized 1,4-dihydropyridine/pyridine compounds bearing tetrazole and 1,3,4-oxadiazole groups by using Hantzsch method and characterized by FT-IR spectroscopy, elemental analysis, and ¹H and ¹³C NMR and studied PK activation, ADME, and molecular docking. The studies revealed that all original synthesized compounds activated PK and AC₅₀ (half-maximal activating concentration) values of the compounds were extremely effective (1.30 μM to 14.65 μM).

Keywords: Rabbit Muscle Pyruvate Kinase, Tetrazole, 1,3,4-oxadiazole

INTRODUCTION

Pyruvate kinase (PK, EC: 2.7.1.40) is recognised as a crucial mechanism in the metabolic pathway that generates energy for cells. There are four major PK isozymes of pyruvate kinase in mammals, and these are generally

^a Kocaeli University, Faculty of Arts and Science, Chemistry Department, Umuttepe Campus, Kocaeli, Turkey

^b Duzce University, Scientific and Technological Research Laboratory, Konuralp Campus, Duzce, Turkey

^c Sakarya University, Faculty of Science, Chemistry Department, Esentepe Campus, Serdivan, Sakarya, Turkey

^d Batman University, Technical Sciences Vocational School, Veterinary Science Department, Raman Campus, Batman, Turkey

* Corresponding author: oguzhan.kaya@kocaeli.edu.tr



associated with type M1, which is related to muscle, heart and brain, type L, which is related to liver, type R, which is related to red cells and type M2, which is related to early fetal tissues as well as most cancer cells. The PKM1 isoform is expressed in tissues of adults and eliminates the M2 isoform following birth. In comparison with M2, this isoform has powerful pyruvate kinase activity on its own as well. As is, action occurs without allosteric activation with D-fructose-1,6-bisphosphate (FBP). PK is known to generate ATP, the primary source of energy within the cell [1,2]. Accordingly, PK activation is known to be influenced (regulated) by several factors, including the availability of ATP, hormones, and metabolic intermediates. This contributes to balancing the energy demand in the body and when a high energy demand is needed, the PK enzyme is activated to meet this demand [3]. The activity of PK is generally known to be responsible for regulating the energy status of cells so that they can fulfil their functions and maintain cellular energy homeostasis [4]. From a health perspective, PK deficiency is a hereditary disorder caused by mutations in the gene encoding the enzyme. One of the best examples of this is hemolytic anaemia. Anaemia is known to cause a serious decrease in PK activity as it causes metabolic abnormalities [5]. It may induce symptoms that include weariness, jaundice, and muscle weakness, as well as muscle cramps, pain, and an increased risk of injury [6]. Furthermore, to how it functions in PK deficit, the drop-in PK activity with aging has been related with sarcopenia, a natural loss of muscular mass and strength [7]. Furthermore, some types of cancer may have altered PK activity which can affect their energy metabolism and contribute to their growth and survival. Finally, it is known to be affected in heart diseases such as heart failure, which can affect energy production in heart cells and contribute to disease progression [8]. Given these total conditions, changes in PK activity can have important effects on energy metabolism and contribute to the development and arrest of various diseases and conditions [9-11].

Tetrazoles are five-membered heterocyclic compounds containing four nitrogen atoms and one carbon atom in the ring structure and oxadiazoles are known as five-membered heterocyclic compounds containing one nitrogen atom, two oxygen atoms and two carbon atoms in the ring structure [12, 13]. Nitration of hydrazine [14-16], cyclisation of nitriles [17-19] and azidation of nitriles [19-22] are the most well-known methods used for the synthesis of tetrazoles. Oxadiazoles are synthesized by the reaction of nitriles with diazonium salt or isocyanate, reaction of carboxylic acids with hydrazine or hydrazides or reaction of amides/nitriles with isocyanate or diazonium salt [23-25]. Tetrazoles are known for their stability and high explosive potential and used in military applications [26]. They are also used in pharmaceuticals as active ingredients in some drugs [27], including anti-ulcer [28], anti-fungal [29]

and anti-tumour [30,31] drugs. Oxadiazoles are used in various applications in medicinal chemistry, including anti-proliferative [32], anti-tumour [33, 34], anti-thrombotic [35] and anti-microbial agents [36, 37], as well as the active ingredient in some herbicides [38] and in the synthesis of composite materials due to their high thermal stabilities and electrical conductivities [39].

Tetrazole and oxadiazole chemical compounds have been found to have a variety of effects on pyruvate kinase. Tetrazole was discovered to mobilize the enzyme under pressure, and the presence of K^+ , Mg^{2+} , and ADP offered additional protection [40]. Oxadiazole, on the other hand, has been demonstrated to have a twofold impact on liver and erythrocyte pyruvate kinases, serving as an allosteric activator in the absence of fructose 1,6 bisphosphate and a competitive inhibitor in its presence [41]. These findings indicate that both substances may regulate pyruvate kinase activity, potentially influencing its role in glycolysis and other metabolic processes. In addition, investigations have revealed that tetrazole and oxadiazole can alter pyruvate kinase activity by binding to particular locations on the enzyme [42]. This highlights the possibility for tetrazole and oxadiazole to be used as key drugs in the research of the pyruvate kinase enzyme mechanism, modulating enzyme activity and regulation.

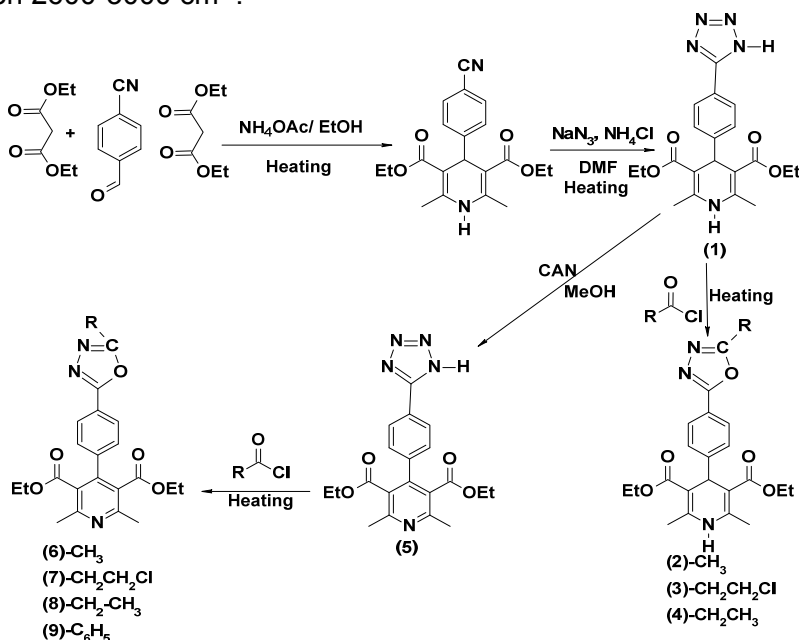
This study was designed on the basis of the good results of our previously synthesized ureido phenyl substituted 1,4-dihydropyridines on pyruvate kinase [43]. The 1,4-dihydropyridine/pyridine compounds with tetrazole and 1,3,4-oxadiazole groups were produced and described. *In vitro* studies demonstrated that these compounds have activatory effects on PK. The chemical features of the produced compounds were examined in computational molecular modeling. Additionally, drug-likeness score, bio-based RO5, docking of molecular structures with PK, and frontier molecular orbitals (ΔE , LUMO-HOMO gap) were calculated. The goal is to detect possible new medication substances that are active for the therapy of cancer and muscle-related sickness by activating the PK with synthetically produced substances.

RESULTS AND DISCUSSION

4-cyanophenyl-1,4-dihydropyridine compound was synthesized in a high yield by the Hantzsch method using 4-cyano benzaldehyde, ethyl acetoacetate, ammonium acetate and L-proline as a catalyst. Firstly, the tetrazole compounds were obtained with NaN_3-NH_4Cl in DMF at $140^\circ C$ for overnight. Then, Oxadiazole substituted-1,4-dihydropyridine and 2,6- dimethylpyridine derivatives were successfully synthesized with reacting acid chlorides and tetrazole compounds by heating and shown in scheme 1.

In the ^1H NMR spectrum of the 4-cyanophenyl-1,4-dihydropyridine compound, the hydrogen atom attached to the nitrogen atom at the position 1 resonances as a singlet around 6.0 ppm due to the electronegativity of nitrogen, while the hydrogen atom at the position 4 resonances around 5.0 ppm. The protons of the aromatic ring containing nitrile group at the fourth position are seen as doublet at 7.4 and 7.6 ppm. In the IR spectra, nitrile stretching is observed in the 2230 cm^{-1} . The peak of the carbon atom of the nitrile was observed at 119 ppm in the ^{13}C NMR.

While obtaining tetrazole compound from 4-cyanophenyl-1,4-dihydropyridine compound, azide–nitrile 1,3-dipolar cycloaddition reaction was carried out. In the tetrazole compound, while the hydrogen atom attached to the nitrogen atom at the position 1 was seen as a singlet around 6.0 ppm in the ^1H NMR, nitrile stretching peak was disappeared in the 2230 cm^{-1} in IR and the peak of carbon atom of the nitrile was not seen any more at 119 ppm in the ^{13}C NMR. Hydrogen atom of the tetrazole ring was not observed in ^1H NMR due to its acidity. However, the chemical shifts of the doublets of the aromatic ring attached to the tetrazole ring shifted to the downfield due to the tetrazole ring and resonance as two doublets between 7.40 and 8.00 ppm. In addition, the specific stretching peak of the tetrazole ring in IR was observed between $2600\text{--}3000\text{ cm}^{-1}$.

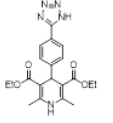
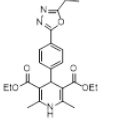
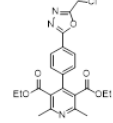
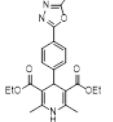
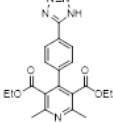
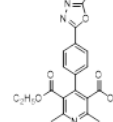
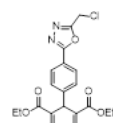
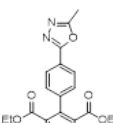
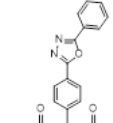


Scheme 1. Synthesis of tetrazole and 1,3,4-oxadiazole substituted 1,4-dihydropyridine

The compound (1) was oxidized with cerium (IV) ammonium nitrate (CAN) in methanol at room temperature to obtain an aromatized pyridine compound containing tetrazole. When the ^1H NMR values of the compound (5) was examined, the hydrogen atom attached to the nitrogen atom at the position 1 and hydrogen atoms at the position 4 were not seen any more due to aromatization of the 1,4-dihydropyridine ring. For the 1, 3, 4-oxadiazole compounds for example the compound (6), two different carbon peaks were observed in ^{13}C NMR. One is for the oxadiazole ring at around 165 ppm and the other is methyl at around 25 ppm.

Activation effect on rabbit muscle PK is demonstrated *in vitro*. The study was carried out on nine organic substances containing 1,4-dihydropyridine/pyridine compounds including tetrazole and oxadiazole, with AC_{50} values between 1.30 μM and 14.65 μM . The AC_{50} values for tetrazole and oxadiazole compounds containing 1,4-dihydropyridine/pyridine is given in Table 1.

Table 1. AC_{50} result of tetrazole and 1,3,4-oxadiazole compounds

Structure	AC_{50} (μM)	Structure	AC_{50} (μM)	Structure	AC_{50} (μM)
 1	2.01	 4	3.73	 7	1.79
 2	1.62	 5	10.31	 8	6.05
 3	1.30	 6	14.65	 9	9.76

According to the results shown in Table 1, the activators used in this study exhibited the values in the range of 1.30 μM - 14.65 μM and were shown to exhibit better activation than N-(4-Chloro-3-fluorophenyl)-7-fluoro-2-oxo-1,2,3,4-tetrahydroquinoline-6-sulfonamide (90 μM) [44], DASA-10 (10 μM), TEPP-46 (79.5 μM) [45], which are the best-known activators in the literature.

However, although it was observed that 1,4 dihydropyridine derivatives containing 1, 3, 4-oxadiazole showed higher activation than 1,4-dihydropyrimidine, both types of compounds have good activation when the chlorine group is bound on the 1,3,4- oxadiazole structure ((7) = 1.79 μM and (3) = 1.30 μM). But, 1,3,4-oxadiazole with an ethyl group on it was 3,73 μM for (4) and 6,05 μM for compound (8), indicating that 1,4 dihydropyridine was almost twice active in the activation value. While the methyl (6) and benzyl (9) groups bearing 2,6-dimethylpyridine structure exhibited AC_{50} values of 14.65 μM and 9.76 μM respectively, the results in the form methyl (2) groups of 1, 4 dihydropyridine structures were 1.62 μM , approximately nine times lower AC_{50} values. All results are supported by the recent use in the literature of activators such as AMPK ($\alpha 1\beta 1\gamma 1$) [46], Nrf2 activator [47] and Caspase-3 [48] with oxadiazole compounds.

Pharmacokinetic properties prediction

ADME (Absorption, Distribution, Metabolism and Excretion) plays an important role in the evaluation of whether organic molecules can be active pharmaceutical ingredients. Because thanks to the results evaluated as a result of ADME studies, many organic molecules are eliminated before *in vitro* and *in vitro* studies. The tetrazole and oxadiazole compounds designed and synthesised by us were evaluated mutually via SwissADME, Molsoft and Molinspiration. These results were shown in Table 2. The evaluation was based on water solubility (MolLogS), octanol water partition (MolLogP), hydrogen bond acceptors (HBA), hydrogen bond donors (HBD), total surface area (TPSA), the blood-brain barrier (BBB) and drug-likeness score. All results are presented in Table 2. The molecular weight of tetrazole and 1,3,4-oxadiazole compounds were found to be 395.41 g/mol and 473.52 g/mol, which fulfils the RO5 rule of molecular weight less than 500. The solubility of the molecules in water was found to be between 2.46 and 5.18 moderate to poor. Drug similarity scores ranged from -0.14 to 0.34, indicating potential drug active ingredient. The BBB Score is computed utilizing statistical assessments of the number of aromatic rings, MWHBN (a combination of molecular weight, hydrogen bond donor, and hydrogen bond acceptor), heavy atoms, topological polar surface area, and pKa. The scores for each of the nine molecules varied between 1.58 to 2.61, signifying a medium value (6-High, 0-Low). [49].

The synthesized two-tetrazole and seven-oxadiazole compounds fulfilled all the pharmacokinetic properties required by the Lipinski rule [50]. Again, all molecules fulfil the requirements of Veber's rule, HBA number should be less than 10, polar surface area should be <140 and molecular weight should be <500 [51]. By fulfilling $1 \geq \log P \leq 6$ and $0 \geq \text{tPSA} \leq 132 \text{ \AA}^2$,

all compounds satisfied the Egan rule. Drug similarity regulates for the Ghose rule should be demonstrated to be between 20 and 70 total atomic numbers, molecular weight 160 to 480, log P -0.4 to 5.6, and molar refraction 40 to 130. Complete the rule and compare it to all compounds [52, 53]. Furthermore, the Muegge rule was looked into, and it became apparent that all created ligands entirely fulfilled the rule. A comparison of all compounds is provided in Table 2.

Table 2. ADME result of synthesized compounds

Ligands	1	2	3	4	5	6	7	8	9
No. HBA	7	7	7	7	8	8	7	7	7
No. HBD	2	1	1	1	1	0	1	2	1
Num. rotatable bonds	8	8	9	9	8	8	9	8	9
MolLogP (mg/L)	2.46	2.78	3.38	3.56	3.03	3.35	3.96	2.46	5.18
MolLogS (mg/L)	-2.77	-3.11	-3.40	-3.52	-3.39	-3.56	-4.49	-2.77	-5.30
Molar Refractivity	108.4	113.5	118.3	118.3	104.9	110.0	118.3	108.4	118.3
TPSA(Å ²)	103.55	103.55	103.55	103.55	103.55	104.41	103.55	103.55	103.55
Mol. Vol. (A ³)	418	445	456	462	384	411	422	418	463
Drug Likeness Score	0.23	0.25	0.17	0.28	-0.11	-0.13	-0.14	0.23	0.01
Synthetic accessibility	4.19	4.39	4.41	4.55	3.19	3.47	4.56	4.19	4.56
BBB Score	2.36	2.61	2.56	2.56	2.06	2.31	2.26	2.36	1.58
pKa of most Basic/Acidic group	-1.24 / 3.51	-1.24 / 4.97	-1.24 / 4.97	-1.24 / 4.98	-0.48 / 3.70	-0.48 / 24.80	-0.48 / 22.71	-1.24 / 3.51	-0.48 / 24.80

HOMO-LUMO levels

In molecular orbital theory, The HOMO-LUMO (Highest Occupied Molecular Orbital - Lowest Occupied Molecular Orbital) computation analyzes the electronic structure and reactivity of molecules. Table 3 illustrates the results of theoretical DFT calculations for nine novel compounds. Based on the research, a small HOMO-LUMO gap increases the molecule's susceptibility to chemical processes because transporting an electron from HOMO to LUMO needs less energy [54–57]. The larger the gap, the more energy needs to be transferred to move an electron to the LUMO, making the molecule less reactive. Compound (1) has the highest activity ($E=4.01$ eV), whereas compound (5) has the lowest activity ($E=5.13$ eV).

Examination of Table 3 reveals that the molecular LUMO-HOMO range (ΔE) is between 4.01 eV and 5.13 eV. Therefore, although the results seem to be very close to each other, the highest reactivity was observed in compound (1) and compound (9), while the lowest reaction reactivity was observed in compound (5). Furthermore, from the boundary orbital representation in Table 3, the molecules exhibited electrophilic attacks on atoms with HOMO orbitals (positive charges or atoms) and nucleophilic attacks on atoms with LUMO orbitals (negative charges or electrons).

Table 3. HOMO. LUMO. IP. EA and ΔE (LUMO-HOMO gap) data for synthesized compounds

Compound	HOMO eV	LUMO eV	ΔE (LUMO-HOMO gap)	Ionization potential (IP) eV	Electron affinity (EA) eV
1	-5.46	-1.45	4.01	-5.46	-1.45
2	-5.45	-1.25	4.20	-5.45	-1.25
3	-6.45	-2.00	4.46	-6.45	-2.00
4	-6.85	-2.01	4.84	-6.85	-2.01
5	-7.07	-1.94	5.13	-7.07	-1.94
6	-5.43	-1.23	4.20	-5.43	-1.23
7	-5.50	-1.29	4.21	-5.50	-1.29
8	-6.65	-1.82	4.83	-6.65	-1.82
9	-5.46	-1.43	4.04	-5.46	-1.43

Table 3 is also researched. The theoretical ionization potential (IP) using negative HOMO energies and possible electron affinity (EA) values using negative LUMO energies have been estimated (Koopman's theorem) [58].

Molecular docking and structure activity relationship (SAR) study

This molecular docking evaluation was performed on the PK (PDB:1PKN) via the Swiss Dock docking server [59, 60]. The evaluation of the docking results and the selection of the structure with the best value were performed via UCSF chimera [61]. Various insertion parameters such as fullfitness (FF), van der Waals energy (ΔG_{vdw}), $\Delta G_{lignolvpol}$ and Gibbs free energy (ΔG) were examined. The determined binding constants are in agreement with the experimental AC_{50} values, indicating a significant correlation between computational predictions and tetrazole, and 1,3,4-oxadiazole compounds experimental observations of the interaction, especially for the direct calculation of the AC_{50} for pyruvate kinase enzyme (Table 4).

Table 4. Molecular docking results of synthesized compounds

Compound	AC_{50} (μM)	ΔG (kcal/Mol)	Fullfitness (FF)	ΔG_{vdw} (kcal/Mol)	$\Delta G_{lignolvpol}$ (kcal/Mol)
1	2.01	-7.75	-3023.03	-41.55	-9.62
2	1.62	-7.45	-3000.90	-36.85	-9.77
3	1.30	-7.82	-2987.46	-59.89	-10.26
4	3.73	-7.27	-2950.90	-33.99	-8.65
5	10.31	-7.85	-2966.07	-60.19	-9.04
6	14.65	-7.26	-2950.90	-33.99	-10,43
7	1.79	-7.97	-2943.40	-53.07	-9.04
8	6.05	-7.88	-2951.21	-39.44	-9.62
9	9.76	-7.88	-2928.07	-39.81	-9.77

Details of the SAR study are given in Table 5, vdW (Van Der Waals) bonds are a critical step in the formation of a stable protein-ligand most active compound. Because vdW interactions are the most effective type of interaction in determining the shape and orientation of organic compounds within the active binding site of the protein [62]. This is the attractive factor that can attract organic substances towards the proteins and allow them to form a more stable complex [63]. In this study, we found that when tetrazole/1,3,4

oxadiazole molecules were near the active site of the PK (1PKN), the electron clouds of the two molecules (acceptor and donor) interacted to form partially positively and negatively charged regions. This formation occurred with a combination of tetrazole/1,3,4-oxadiazole molecules and a variety of residues such as methionine, arginine, proline, tyrosine, glycine and glutamic acid.

Conventional hydrogen bonds are established at molecular docking due to the difference in electronegativity between the nitrogen or oxygen atoms in the tetrazole/1,3,4 oxadiazole and the hydrogen atom of the amino acid residues [64]. These kinds of bonds generally have interaction weaker than covalent bonds, even though they are more powerful than vdW interactions [65]. In the context of protein-ligand interactions, conventional hydrogen bonding was occurred between the PK and the residues Glu A:383 and Glu A:331 for tetrazoles (two molecules) and Arg A:341 and Arg A:338 for oxadiazoles in the seven new molecules.

π -Alkyl and alkyl interactions appear in molecular docking through the attraction between π -electrons on aromatic groups in the structure of organic compounds and alkyl groups in the opposite structure. π -Alkyl and alkyl interactions are much weaker than both traditional hydrogen bonds and vdW interactions, but they are important for stabilization in protein-ligand interactions [66]. The interactions between PK and tetrazoles were observed between Arg A:341, Ala A:348, Pro A:339, Ile A:380, Leu A:379 and Leu A:179 residues, whereas for 1,3, 4-oxadiazoles, it was realized through various residues of the amino acids such as arginine, alanine, proline, isoleucine, leucine and tyrosine.

Amide- π stack interactions are based on the interaction between the π -electrons of tetrazole or 1,3,4-oxadiazole rings and the carbonyl group of amino acid residues [67]. In the current study, the π -donor hydrogen bond interaction between the compound (5) and PK was observed through the Glu A:331 residue, whereas for the compound (2) it was observed through the Arg A:341 residue. The π -donor hydrogen bond interaction between the compound (5) and (4) with PK was mediated by an aliphatic or aromatic CH in the structure of the novel molecule, with the Gln A:328 and Asn A:74 residues acting as hydrogen bond donors.

π -Sigma interactions result in molecular docking via the C-H- π or C=C- π interaction when the π -electron cloud of an aromatic ring interacts with the sigma bond of a nearby atom [68]. It is found between the Ser A:345 residue and the compound (6), the Gly A:344 residue and the compound (2), the (8) with Met A:376 residue of muscle PK.

NOVEL TETRAZOLE AND 1,3,4-OXADIAZOLE DERIVATIVES SYNTHESIS, MOLECULAR DOCKING, ADME, POTENTIAL ACTIVATOR FOR RABBIT MUSCLE PYRUVATE KINASE

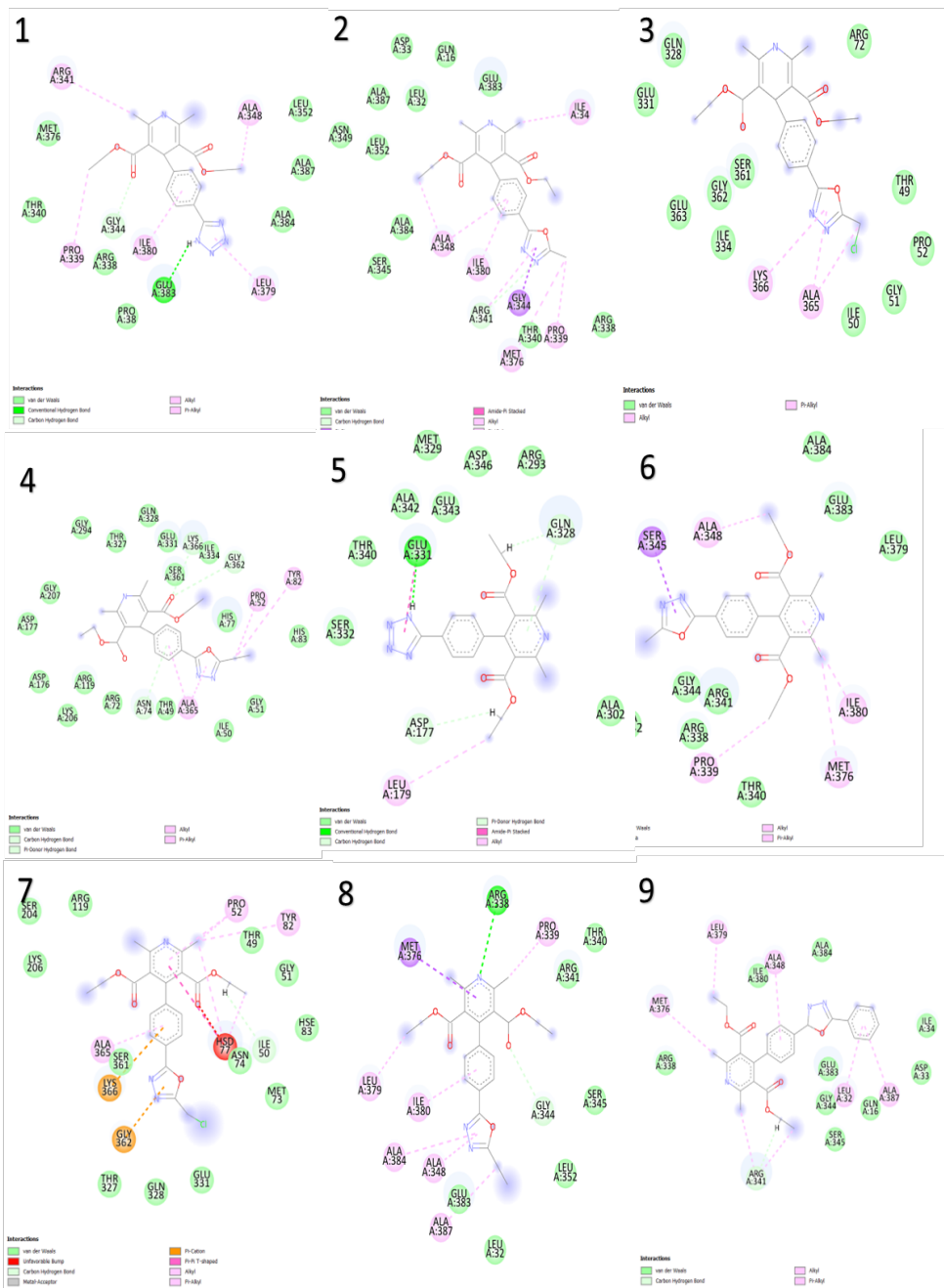


Figure 1. 2D interaction of compounds.

Table 5. Interaction results of synthesized compounds

	1	2	3	4	5	6	7	8	9
Van Der Waals	Met A:376, Thr A:340, Arg A:338, Pro A:38, Ala A:384, Ala A:387, Leu A:352	Ser A:345, Leu A:352, Asn A:349, Ala A:387, Leu A:32, Asp A:33,i Gln A:16, Glu A:383, Arg A:338	Gln A:328, Glu A:331, Ser A:361, Gly A:362, Glu A:363, Ile A:334, Ile A:50, Gly A:51, Pra A:52, Thr A:49, Arg A:72	Asp A:176, Asp A:177, Gly A:207, Gly A:294, Thr A:327, Gln A:328, Glu A:331, Ile A:334, Ser A:361, His A:77, His A:83, Gly A:51, Ile A:50, Thr A:49,	Ser A:332, Thr A:340, Ala A:342, Met A:329, Glu A:343, Asp A:346, Arg A:293, Ala A:302	Ala A:342, Gly A:344, Arg A:341, Arg A:338, Ala A:384, Glu A:383, Leu A:379	Ser A:204, Arg A:119, Lys A:206, Thr A:327, Gln A:328, Ser A:361, Asn A:74, Met A:73, Hsd A:83, Gly A:51, Thr A:49	Glu A:383, Leu A:32, Leu A:352, Ser A: 345, Arg A:341, Thr A:340	Arg A:338, Ile A:380, Ala A:384, Ile A:34, Asp A:33, Glu A:383, Gly A:344, Gln A:16, Asp A:33, Ser A:345
Conventional Hydrogen band	Glu A:383	Arg A:341	-	-	Glu A:331	-	-	Arg A:338	-
π-Alkyl and Alkyl	Arg A:341, Ala A:348, Pro A:339, Ile A:380, Leu A:379	Ala A:348, Ile A:380, Pro A:339, Met A:376, Ile A:34	Lys A:366, Ala A:365	Ala A:365, Pro A:352, Tyr A:82	Leu A: 179	Ile A:380, Met A:376, Ala A:348,Pro A:339	Tyr A:82, Pro A:52, Ala A:365	Leu A:379, Ile A:380, Ala A:384, Ala A:387, Pro A:339	Ala A:387, Leu A:332, Ala A:348, Leu A:379, Met A:376
Amide -π stacked	-	Arg A:341	-	-	Glu A:331	-	-	-	-
π-Donor hydrogen	-	-	-	Asn A:74	Gln A:328	-	-	-	-
π-Sigma	-	Gly A:344	-	-	-	Ser A:345	-	Met A:376	-
Carbon Hydrogen	Gly A:344	-	-	Lys A:366, Gly A:362	Gln A:328	-	Ile A:50	Gly A:334	Arg A:341
π-Cation	-	-	-	-	-	-	Lys A:366, Gly A:362	-	-
π- π T Shaped	-	-	-	-	-	-	Hsd A:77	-	-

CONCLUSIONS

This work was carried out to discuss the synthesis, characterization, computational analysis and *in vitro* activation study of novel nine compounds. The highest effect of the tetrazole and 1,3,4-oxadiazole substituted 1,4-dihydropyridine compounds were found to be 1.30 μM for the compound (3), while the compound (7) containing another chlorine functional group substituted 2,6-dimethylpyridine showed a very good result with 1.79 μM . Again, considering the whole study, it was observed that the AC50 values of 1,4- dihydropyridines were much higher than 2,6-dimethylpyridine. However, it was shown that all of the newly synthesized derivatives (1-9) have a very good activation potential against PK (1.30 μM -14.65 μM).

The molecular docking results of the nine new compounds synthesized for PK activation showed that the predicted ΔG values were close to each other (-7.27 and -7.97) and the $\Delta\text{G}_{\text{vdw}}$ value was in the range of -39.33 to -60.19. The software Orca 5.0.2 was used to determine the HOMO-LUMO values, ionization potential, electron affinity and the most stable conformation of the compound using molecular mechanics and the B3LYP technique. The most reactive molecule was found to be compound (1) ($\Delta\text{E}=4.01\text{eV}$).

The specific isoform of PK expressed in muscle tissue and is a key enzyme involved in the final step of glycolysis to generate energy in the form of ATP. So, it will be a pioneering result for many studies that muscle PK may also be involved in other cellular processes such as gene expression and cell proliferation.

EXPERIMENTAL SECTION

FT-IR spectra were collected using a SHIMADZU Prestige-21 (200 VCE) spectrometer via an ATR. The ^1H and ^{13}C NMR spectra were acquired with spectrometers set to 300 and 75 Hz on the VARIAN Infinity Plus, correspondingly. The chemical shifts ^1H and ^{13}C are referring to the internal deuterated solvent. A Thermo Scientific Flash 2000 instrument was used for the elemental analysis. Sigma Chem. Co. provided the materials used, which included ethyl acetoacetate, 4-cyanobenzaldehyde, ammonium acetate, and protein assay reagents. All of the chemicals used were of the analytical grade.

1,4-Dihydropyridine Synthesis; 4-Cyanobenzaldehyde (5.0 mmol), ethyl acetoacetate (10.0 mmol), ammonium acetate (5.0 mmol) and L-proline as a catalyst were dissolved in methanol (5 mL) and stirred for 6 hours at

80 °C in a flask. At the end of the reaction, the reaction mixture was allowed to cool to room temperature and poured into 100.0 mL of ice-cold water and stirred. The precipitate was filtered off and dried. The product was purified by crystallisation from ethanol. The structural analysis of the product was confirmed by ¹H, ¹³C NMR and FTIR spectra.

Tetrazole Synthesis: To the solution of nitrile compound (5.0 mmol) in Dimethylformamide (DMF, 5 mL), sodium azide (20.0 mmol) and ammonium chloride (20.0 mmol) were added and heated overnight at 140 °C in a flask. At the end of the reaction, the reaction mixture was allowed to cool to room temperature and poured into 100.0 mL of ice-cold water and stirred. HCl was used to adjust the pH of solution to 1. The precipitate was filtered off and dried. The product was purified by crystallisation from acetone/hexane. The structural analysis of the product was confirmed by ¹H, ¹³C NMR and FTIR spectra.

Aromatization of 1,4-Dihydropyridine compounds: 1,4-dihydropyridine derivative (1 mmol) in 5.0 mL of water was dissolved. MeOH and NH₄SCN (1.20 mmol) were added to the solution and then stirred. Solution of 2.0 mmol CAN in MeOH (10 mL) was added to the reaction mixture by dropwise over 30 minutes using the dropping funnel and the mixture was stirred for two hours at room temperature. The reaction mixture was then poured into 100.0 mL of water and extracted with dichloromethane. The organic phase was washed three times with water and dried with sodium sulphate. Dichloromethane was removed using a rotary evaporator. The product was purified by crystallisation from acetone/hexane. The structural analysis of the product was confirmed by ¹H, ¹³C NMR and FTIR spectra.

Oxadiazole Synthesis: Tetrazole derivatives (1.0 mmol) were dissolved in 2.0 mL of acyl chloride and heated overnight at 100 °C under an inert atmosphere. The reaction mixture was then poured into 100 mL of water and extracted with dichloromethane. The organic phase was washed three times with water and dried with sodium sulphate. Dichloromethane was removed using a rotary evaporator. The product was purified by crystallisation from acetone/hexane. The structural analysis of the product was confirmed by ¹H, ¹³C NMR and FTIR spectra.

Diethyl 4-(4-(1H-tetrazol-5-yl)phenyl)-2,6-dimethyl-1,4-dihydropyridine-3,5-dicarboxylate (1): M.p. 100.8 °C, ¹H NMR (300 MHz, CDCl₃): 8.18 (2H, d, Ar-H), 7.62 (2H, d, Ar-H), 6.66 (1H, s, NH), 4.99 (1H, s, CH), 4.00 (2x2H, q, CH₂), 2.39 (2x3H, s, CH₃), 1.47 (2x3H, t, CH₃). ¹³C NMR (75 MHz): 166.7, 164.2, 164.4, 145.8, 139.0, 129.5, 128.5, 127.6, 121.6, 62.6, 22.7, 19.0, 11.74. FT-IR ν (cm⁻¹): 3024.89 (Ar-H), 2939.52 (Aliphatic-H), 1722.43(C=O),

1656.77(C=O), 1500.62 (N=N). Chemical Formula: $C_{20}H_{23}N_5O_4$, Elemental Analysis (Calculated): C, 60.44; H, 5.83; N, 17.62; O, 16.10, (Found): C, 60.21; H, 5.94; N, 17.50.

Diethyl-2,6-dimethyl-4-(4-(5-methyl-1,3,4-oxadiazol-2-yl)phenyl)-1,4-dihydropyridine-3,5-dicarboxylate (2): M.p. 126.8°C, 1H NMR (300 MHz, $CDCl_3$): 7.81 (2H, d, Ar-H), 7.47 (2H, d, Ar-H), 6.82 (1H, s, NH), 5.09 (1H, s, CH), 4.05 (2x2H, q, CH_2), 2.75 (3H, s, CH_3), 2.61 (2x3H, s, CH_3), 1.33 (2x3H, t, CH_3), ^{13}C NMR (75 MHz, $CDCl_3$): 167.7, 165.4, 163.7, 152.5, 145.3, 145.3, 129.2, 126.5, 121.5, 103.3, 60.0, 40.3, 19.4, 14.5, 11.3. FT-IR ν (cm^{-1}): 3275.13 (N-H), 3097.89 (Ar-H), 2983.88 (Aliphatic-H), 1691.57 (C=O), 1651.07 (C=O), 1498.69 (N-N). Chemical Formula: $C_{22}H_{25}N_3O_5$. Elemental Analysis (Calculated): C, 64.22; H, 6.12; N, 10.21; O, 19.44, (Found): C, 64.56; H, 6.21; N, 10.04.

Diethyl-4-(4-(5-(chloromethyl)-1,3,4-oxadiazol-2-yl)phenyl)-2,6-dimethyl-1,4-dihydropyridine-3,5-dicarboxylate (3): M.p. 87.8°C, 1H NMR (300 MHz, $CDCl_3$): 7.92 (2H, d, Ar-H), 7.48 (2H, d, Ar-H), 6.02 (1H, s, NH), 5.03 (1H, s, CH), 4.95 (2H, s, CH_2Cl), 4.06 (2x2H, q, CH_2), 2.39 (2x3H, s, CH_3), 1.21 (2x3H, t, CH_3). ^{13}C NMR (75 MHz, $CDCl_3$): 167.5, 162.0, 152.5, 144.8, 139., 129.1, 127.5, 121.4, 103.6, 60.1, 46.1, 19.8, 14.5. FT-IR ν (cm^{-1}): 3307.92 (N-H), 2980.09 (Aliphatic-H), 1691.15 (C=O), 1678.07 (C=O), 1485.19 (N-N), 1205.51 (C-O-C). Chemical Formula: $C_{22}H_{24}ClN_3O_5$, Elemental Analysis (Calculated): C, 59.26; H, 5.43; Cl, 7.95; N, 9.42; O, 17.94, (Found): C, 59.42; H, 5.51; N, 9.66.

Diethyl-4-(4-(5-ethyl-1,3,4-oxadiazol-2-yl)phenyl)-2,6-dimethyl-1,4-dihydropyridine-3,5-dicarboxylate (4): M.p. 99.6°C, 1H NMR (300 MHz, $CDCl_3$): 9.22 (NH, s), 7.89 (2H, d, Ar-H), 7.40 (2H, d, Ar-H), 6.02 (1H, s, NH), 5.15 (1H, s, CH), 4.08 (2x2H, q, CH_2), 2.93 (2H, q, CH_2), 2.39 (2x3H, s, CH_3), 1.48 (3H, t, CH_3), 1.20 (6H, t, CH_3), ^{13}C NMR (75 MHz, $CDCl_3$): 167.8, 165.2, 152.4, 145.36, 129.0, 128.5, 121.6, 103.3, 60.6, 40.2, 21.2, 19.3, 14.9, 11.0. FT-IR ν (cm^{-1}): 3304.05 (N-H), 2980.08 (Aliphatic-H), 1678.02 (C=O), 1651.07 (C=O), 1487.12 (N-N). Chemical Formula: $C_{23}H_{27}N_3O_5$, Elemental Analysis (Calculated): C, 64.93; H, 6.40; N, 9.88; O, 18.80, (Found): C, 65.02; H, 6.56; N, 9.69.

Diethyl-4-(4-(1H-tetrazol-5-yl)phenyl)-2,6-dimethylpyridine-3,5-dicarboxylate (5): M.p. 141.3°C, 1H NMR (300 MHz, $CDCl_3$): 8.21 (2H, d, Ar-H), 7.42 (2H, d, Ar-H), 4.05 (4H, q, CH_2), 2.69 (2x3H, s, CH_3), 0.90 (2x3H, t, CH_3), ^{13}C NMR (75 MHz, $CDCl_3$): 167.6, 158.0, 155.9, 145.9, 139.3, 129.3, 127.3, 125.4, 62.1, 22.7, 13.8. FT-IR ν (cm^{-1}): 3096.78 (Ar-H), 2989.66 (Aliphatic-H), 2868.75, 1722.43 (C=O), 1556.20, Chemical Formula: $C_{20}H_{21}N_5O_4$, Elemental

Analysis (Calculated): C, 60.75; H, 5.35; N, 17.71; O, 16.19, (Found): C, 60.24; H, 5.41; N, 17.88.

Diethyl-2,6-dimethyl-4-(4-(5-methyl-1,3,4-oxadiazol-2-yl)phenyl)pyridine-3,5-dicarboxylate (6): M.p. 90.2°C, ¹H NMR (300 MHz, CDCl₃): 8.15 (2H, d, Ar-H), 7.52 (2H, d, Ar-H), 4.00 (4H, q, CH₂), 2.69 (2x3H, s, CH₃), 2.65 (3H, s, CH₃), 0.90 (2x3H, t, CH₃), ¹³C NMR(75 MHz, CDCl₃): 167.6, 164.5, 164.2, 155.9, 145.1, 140.1, 129.1, 127.1, 126.8, 124.9, 61.7, 23.0, 13.83, 11.29. FT-IR v (cm⁻¹): 3064.89 (Ar-H), 2980.66 (Aliphatic-H), 1720.22 (C=O), 1682.77 (C=O), 1556.55. Chemical Formula: C₂₂H₂₃N₃O₅, Elemental Analysis (Calculated): C, 64.54; H, 5.66; N, 10.26; O, 19.54, (Found): C, 64.25; H, 5.71; N, 10.42.

Diethyl-4-(4-(5-(chloromethyl)-1,3,4-oxadiazol-2-yl)phenyl)-2,6-dimethylpyridine-3,5-dicarboxylate (7): M.p. 81.5°C, ¹H NMR (300 MHz, CDCl₃): 8.11 (2H, d, Ar-H), 7.57 (2H, d, Ar-H), 4.89 (2H, s, CH₂), 4.01 (2x2H, q, CH₂), 2.59 (2x3H, s, CH₃), 1.00 (2x3H, t, CH₃). ¹³C NMR (75 MHz, CDCl₃): 167.6, 165.6, 162.6, 156.0, 145.0, 140.0, 129.3, 127.5, 126.9, 126.7, 123.5, 61.7, 33.1, 23.1, 13.9. FT-IR v (cm⁻¹): 3064.89 (Ar-H), 2980.66 (Aliphatic-H), 1720.52 (C=O), 1697.37 (C=O), 1556.66 (N-N). Chemical Formula: C₂₂H₂₂ClN₃O₅, Elemental Analysis (Calculated): C, 59.53; H, 5.00; Cl, 7.99; N, 9.47; O, 18.02, (Found): C, 59.88; H, 5.20; N, 9.65.

Diethyl-4-(4-(5-ethyl-1,3,4-oxadiazol-2-yl)phenyl)-2,6-dimethylpyridine-3,5-dicarboxylate (8): M.p. 100.8°C, ¹H NMR (300 MHz, CDCl₃): 8.18 (2H, d, Ar-H), 7.62 (2H, d, Ar-H), 4.00 (2x2H, q, CH₂), 2.99 (2H, q, CH₂), 2.39 (2x3H, s, CH₃), 1.47 (3H, t, CH₃), 1.24 (2x3H, t, CH₃). ¹³C NMR (75 MHz, CDCl₃): 166.7, 164.2, 164.4, 145.8, 139.0, 129.5, 128.5, 127.6, 121.6, 62.6, 22.7, 19.0, 11.7. FT-IR v (cm⁻¹): 3024.89 (N-H), 2939.52 (Aliphatic-H), 1722.43 (C=O), 1656.77 (C=O), 1500.62 (N-N). Chemical Formula: C₂₃H₂₅N₃O₅, Elemental Analysis (Calculated): C, 65.24; H, 5.95; N, 9.92; O, 18.89, (Found): C, 65.56; H, 6.11; N, 10.08.

Diethyl-2,6-dimethyl-4-(4-(5-phenyl-1,3,4-oxadiazol-2-yl)phenyl)pyridine-3,5-dicarboxylate (9): M.p. 130.9°C, ¹H NMR (300 MHz, CDCl₃): 8.11 (2H, d, Ar-H), 7.48 (2H, d, Ar-H), 7.32 (2H, d, Ar-H), 7.30 (2H, d, Ar-H), 7.25 (H, t, Ar-H), 4.05 (2x2H, q, CH₂), 2.39 (2x3H, s, CH₃), 1.37 (2x3H, t, CH₃). ¹³C NMR (75 MHz, CDCl₃): 167.9, 165.0, 164.4, 148.6, 139.6, 129.7, 129.1, 128.6, 128.1, 127.6, 127.3, 125.9, 119.5, 60.7, 19.3, 14.39. FT-IR v (cm⁻¹): 3038.89 (Ar-H), 2980.02 (Aliphatic-H), 1722.43 (C=O), 1548.84, 1487.12 (N-N). Chemical Formula: C₂₇H₂₅N₃O₅, Elemental Analysis (Calculated): C, 68.78; H, 5.34; N, 8.91; O, 16.97, (Found): C, 68.52; H, 5.18; N, 9.06.

HOMO-LUMO levels

The theoretical computations and geometrical optimization for the examined junctions were carried out using the open source DFT code, ORCA package version 5.0.2 [69], on an overclocked Intel®core i5-6400 CPU (2.71 GHz) with 8 GB RAM. Density functional theory B3LYP [70-73] is used as D3 zero [74] with dispersion correction and a damping function proposed by Becke and Johnson with a basis set (def-2-SVP) [75, 76]. Because there are no imaginary frequencies, the equilibrium geometry has a real minimum on the potential energy surface (PES).

PK Activity Assay

PK activity was assessed by measuring pyruvate subsequent generations, which was later measured by oxidization of NADH in the absence of excessive lactate dehydrogenase [2, 77]. The following reaction components (final concentrations) were added to a spectrophotometric cuvette (1 mL): 50 mM Tris-HCl buffer, pH 7.4; 100 mM KCl; 10 mM MgCl₂; 2 mM ADP; 1 mM PEP; 0.2 mM NAD-H; 8 un/mL LDH. The addition of PK preparation started the reaction (0.02–0.04 units). A decrease in optical density was registered at 340 nm on a spectrophotometer. Thermo Scientific Evolution 201 UV-Visible Spectrophotometer (Driesch, Germany). Activation effects of the novel compounds on enzyme activities were tested under *in vitro* conditions.

In vitro activation studies

Several amounts of these substances were added to the enzyme reaction mixture for the activation tests of nine compounds. Without a solution containing produced chemicals, PK activity was assumed to be 100%. Regression analysis was used in conjunction with the Microsoft Office Excel program to determine the activity percentage values of PK for various concentrations of each tetrazole and 1,3,4 oxadiazole. Table 1 contains the AC₅₀ values that were determined from Lineweaver-Burk [78] graphs.

Molecular preparation of the structures

The 2D structures of the ligands were drawn using ACD chemsketch software. Iterative runs of Avogadro 1.9.0. through a shell script provided the primary 3D generation of the structures as mol2 format [79]. The shell script was provided by means of batch scripting in the Windows operating system. The 3D crystal structures for four PK isozymes, 1PKN, were retrieved from RCSB protein data bank [80]. Water molecules and the co-crystal ligands

were thereafter excluded from the structures and the PDBs were corrected in terms of missing atom types and application program interface (Discovery studio 2020 Client) was applied for generation and running of 2D interaction [81].

Pharmacokinetic properties prediction

Pharmacokinetic characteristics in computer-assisted drug design (CADD) are a significant component of drug discovery since they assist determine if a drug candidate should be tested in a biological system. PK characteristics aid in and explain the integrity & efficacy of compounds throughout the early phases of drug development. Therefore, the Swiss ADME, Molsoft and Molinspiration were used in the study to analyse the pharmacokinetic properties of the novel nine compounds [82-84].

ACKNOWLEDGMENTS

This work was supported by a SCIENTIFIC AND TECHNOLOGICAL RESEARCH INSTITUTION OF TURKEY (TUBİTAK) 2209 Project "Synthesis of Penta Substituted Pyridine Compounds Containing Alkyl/Aryl and Amino Oxadiazole in the 5-Position".

REFERENCES

1. V. Gupta; R.N.K. Bamezai; *Protein Sci.*, **2010**, *19*, 2031-2044.
2. S. Strumilo; A. Tylicki; *Zh. Evol. Biokhim. Fiziol.*, **2015**, *51*,103-7.
3. M. Alquraishi; D.L. Puckett; D.S. Alani; A.S. Humidat; V.D. Frankel; D.R. Donohoe; J. Whelan; A. Bettaieb; *Free Radic. Biol. Med.*, **2019**, *143*,176-192.
4. D. Prasanta; J.Y. Son; A. Kundu; K. S. Kim; Y. Lee; K. Yoon; S. Yoon; B.M. Lee; K.T. Nam; and H.S. Kim. N. Kim; *Int. J. Mol. Sci.*, **2019**, *20*, 5622.
5. P. Bianchi; E. Fermo; B. Glader; *Am. J. Hematol.*, **2019**, *94*,149-161.
6. S. Deane; B. E. Phillips; C. R. G. Willis; D.J. Wilkinson; K. Smith; N. Higashitani; J. P. Williams; N. J. Szewczyk; P.J. Atherton; A. Higashitani; T. Etheridge; *GeroScience*, **2023**, *45*, 1271-1287.
7. J. Y. Jan; D.Kim; N. D. Kim; *Biomedicines*; **2023**, *11* (6), 1635.
8. G.D. Lopaschuk; Q.G. Karwi; R. Tian; A.R. Wende; E.D. Abel; *Circ. Res.*, **2021**, *128*,1487-1513.
9. W.J. Israelsen; M.G.V. Heiden; *Semin. Cell. Dev. Biol.*, **2015**, *43*, 43-51.
10. J. Burns; G. Manda; *Int. J. Mol. Sci.*, **2017**, *18*, 2755-2783.
11. K. Zahra; T. Dey; Ashish, S.P. Mishra; U. Pandey; *Front. Oncol.*, **2020**, *10*, 159.
12. C.X. Wei; M. Bian; G.H. Gong; *Molecules*, **2015**, *20*, 5528-5553.
13. C.G. Neochoritis; T. Zhao; A. Dömling; *Chem. Rev.*, **2019**, *119*, 1970-2042.
14. M. Benz; T.M. Klapötke; T. Lenz; J. Stierstorfer; *Chem. A Eur. J. I*, **2022**, *28*, 10.

15. M. Benz; T.M. Klapötke; J. Stierstorfer; M. Voggenreiter; *ACS Appl. Eng. Mat.*, **2023**, 1, 3-6.
16. M. Benz; T.M. Klapötke; J. Stierstorfer; *Chempluschem.*, **2022**, 87, 9.
17. R.Z. Zhang; R.X. Zhang; S. Wang; C. Xu; W. Guan; M. Wang; *Angew. Chem Int. Ed.*, **2022**, 61, 1.
18. D.R. Mishra; B.S. Panda; M.A. Ahemad; S. Nayak; S. Mohapatra; *ChemistrySelect*, **2022**, 7, 46.
19. F. Celik; M. Arslan; M.O. Kaya; E. Yavuz; N. Gencer; O. Arslan; *Artif Cells Nanomed B.*, **2014**, 42, 58-62.
20. S.J. Wittenberger, B.G. Donner; *J. Org. Chem.*, **1993**, 58, 4139-4141.
21. S. L. Ramos; O.J. Cardoso; *Curr. Org. Chem.*, **2021**, 25, 388-403.
22. M.A.E.A.A.A. El-Remaily; O.M. Elhady; *Appl Organomet Chem.*, **2019**, 33, 8.
23. M. Luczynski; A. Kudelko; *Appl. Sci.*, **2022**, 12, 3756.
24. J.J. Wang; W. Sun; W.D. Jia; M. Bian; L.J. Yu; *J. Enzyme. Inhib. Med. Chem.*, **2022**, 37, 2304-2319.
25. K.D. Patel; S.M. Prajapati; S.N. Panchal; H.D. Patel; *Synth. Commun.*, **2014**, 44, 1859-1875.
26. D. Fischer; T.M. Klapötke; J. Stierstorfer; *Angew. Chem. Int. Edit.*, **2015**, 54, 10299-10302.
27. K. Ferydoon; M. M. Seyed; B.D. Samaneh; A. Z. Mohammad; *Medicon Pharm. Sci.*, **2022**, 2, 04-10.
28. L. L. De Lócio; A. P. S. Do Nascimento; M.B. Santos; J. N.NS. Gomes; Y.M.S. De Medeiros; S.L. Albino; V.L. Dos Santos; R.O. De Moura; *Curr Pharm Des.*, **2022**, 28, 1373-1388.
29. T. Ni; X. Chi; F. Xie; L. Li; H. Wu; Y. Hao; X. Wang; D. Zhang; Y. Jiang; *Eur. J. Med. Chem.*, **2023**, 246, 115007.
30. S. DAS; A. Ghosh; P. Upadhyay; S. Sarker; M. Bhattacharjee; P. Gupta; A. Adhikary; *bioRxiv*, **2022**, 1-10.
31. T. Al-Warhi; A. A. Al-Karmalawy; A. A.; Elmaaty, M. A. Alshubramy; M. Abdel-Motaal; T.A. Majrashi; M. Asem; A. Nabil, W. M.Eldehna, M. Sharaky; *Enzyme. Inhib. Med. Chem.*, **2023**, 38, 176-191.
32. B. Yadagiri; S. Gurralla; R. Bantu; L. Nagarapu; S. Polepalli; G. Srujana; N Jain; *Bioorg. Med. Chem. Lett.*, **2015**, 25, 2220-2224.
33. S. Bajaj; V. Asati; J. Singh; P.P. Roy; *Eur. J. Med. Chem.*, **2015**, 97, 124-141.
34. D. Kumar; S. Sundaree; E.O. Johnson; K. Shah; *Bioorg. Med. Chem. Lett.*, **2009**, 19, 4492-4494.
35. B. Vishwanathan; B.M. Gurupadayya; K. S. Venkata; *Bangladesh J. Pharmacol.*, **2016**, 11, 67-74.
36. M. Bhatt; *Int. J. of Pharm. Sci. and Res.*, **2010**, 1, 172-179.
37. K. Rajeev; R. Meenakshi; M. S. Y. Prabodh; *Int. J. of Pharm. Innov.*, **2011**, 37-55.
38. İ.H. Cığerci; *Pak. J. Agric. Sci.*, **2022**, 59, 207-211.
39. M. G. Mohamed; M. M. Samy; T.H. Mansoure; S.U. Sharma; M.S. Tsai; J. H. Chen; J. T. Lee; S. W. Kuo; *ACS Appl. Energy Mater.*, **2022**, 5, 3677-3688.
40. F. G. De Felice; V. C. Soares; S. T. Ferreira; *J. Biochem.*, **1999**, 260, 163-169.

41. H. Buc; F. Demaugre; J.P. Leroux; *BBRC*, **1978**, *85*, 2, 774-779.
42. A. Veith; B. Moorthy; *Curr Opin Toxicol.*, **2018**, *7*, 44-51.
43. M.O. Kaya; T. Demirci; Ü. Çalişır; O. Özdemir; Y. Kaya; M. Arslan. *Res Chem Intermed*; **2024**, *50*, 437-463.
44. M.J. Walsh; K.R. Brimacombe; H. Veith; J.M. Bougie; T. Daniel; W. Leister; L.C. Cantley; W.J. Israelsen; M.G. Vander Heiden; M. Shen; D.S. Auld; C.J. Thomas; M.B. Boxer. *Bioorg. Med. Chem. Lett.*, **2011**, *21*, 6322-6327.
45. D. Anastasiou; Y. Yu; W.J. Israelsen; J.K. Jiang; M.B. Boxer; B.S. Hong; W. Tempel; S. Dimov; M. Shen; A. Jha; H. Yang; K.R. Mattaini; C.M. Metallo; B.P. Fiske, K.D. Courtney; S. Malstrom; T.M. Khan; C. Kung; A.P. Skoumbourdis; H. Veith; Southall N; M.J Walsh; K.R. Brimacombe; W. Leister; S.Y. Lunt; Z.R. Johnson; K.E. Yen; K. Kunii; S.M. Davidson; H.R. Christofk; C.P. Austin; J. Inglese; M.H. Harris; J.M. Asara; G. Stephanopoulos; F.G. Salituro; S. Jin; L. Dang; D.S. Auld, H.W. Park, L.C. Cantley; C.J. Thomas; M.G. Vander Heiden. *Nat. Chem. Biol.*, **2012**, *8*, 839-847.
46. Z. Xiao; Y. Peng; B. Zheng; Q. Chang; Y. Guo; Z. Chen; Q. Li; G. Hu; *Arch. Pharm. (Weinheim)*, **2021**, *354*, 2000458.
47. L.L. Xu; Y.F. Wu; F. Yan; C.C. Li; Z. Dai; Q. D. You; Z. Y. Jiang; B. Di; *Free Radic. Biol. Med.*, **2019**, *134*, 288-303.
48. S. K. Kashaw; S. Agarwal; M. Mishra; S. Sau; A.K. Iyer; *Curr. Comput. Aided Drug Des.*, **2018**, *15*, 55-66.
49. M. Gupta; H. J. Lee; C. J. Barden; D. F. Weaver; *J. Med. Chem.*, **2019**, *62*, 9824-9836.
50. C.A. Lipinski; F. Lombardo; B. W. Dominy; P.J. Feeney; *Adv. Drug. Deliv. Rev.*, **2001**, *46*, 3-26.
51. D. F. Veber; S. R. Johnson; H.Y. Cheng; B. R. Smith; K. W. Ward; K. D. Kopple; *J. Med. Chem.*, **2022**, *45*, 2615-2623.
52. A. K. Ghose; V. N. Viswanadhan; J. J. Wendoloski; *J. Comb. Chem.*, **1999**, *1*, 55-68.
53. A. K. Ghose; T. Herbertz; R. L. Hudkins; B. D. Dorsey; J. P. Mallamo; *ACS Chem. Neurosci.*, **2012**, *3*, 50-68.
54. P. Y. Ayala; G. E. Scuseria; *J. Chem. Phys.*, **1999**, *110*, 3660-3671.
55. A. Kumer; M. N. Sarker; S. Paul; *Int. J. of Chem. and Tech.*, **2019**, *3*, 26-37.
56. S.Muthu; J. U. Maheswari; *Spectrochim. Acta A. Mol. Biomol. Spectrosc.*, **2012**, *92*, 154-163.
57. L. Li; T. Cai; Z. Wang; Z. Zhou; Y. Geng; T. Sun; *Spectrochim. Acta A. Mol. Biomol. Spectrosc.*, **2014**, *120*, 106-118.
58. T. Koopmans; *Physica*, **1934**, *1*, 104-113.
59. A. Grosdidier; V. Zoete; O. Michielin; *Nucleic Acids Res.*, **2011**, *39*, 270-277.
60. A. Grosdidier; V. Zoete; O. Michielin; *J. Comput. Chem.*, **2011**, *32*, 2149-2159.
61. E. F. Pettersen; T. D. Goddard; C. C. Huang; G. S. Couch; D. M. Greenblatt; E. C. Meng; T.E. Ferrin; *J. Comput. Chem.*, **2004**, *25*, 1605-1612.
62. S. Y. Huang; X. Zou; *Int. J. Mol. Sci.*, **2010**, *11*, 3016-3034.
63. P. L. Kastritis; A. M. J. J. Bonvin; *J. R. Soc. Interface*, **2013**, *10*, 20120835.

64. X. Du; Y. Li; Y. L. Xia; S. M. Ai; J. Liang; P. Sang; X. L. Ji; S.Q. Liu; *Int. J. Mol. Sci.*, **2016**, *17*, 144.
65. L. Marchetti; D. Porciani; S. Mitola; C. Giacomelli; *Front. Mol. Biosci.*, **2022**, 921677.
66. O.S. Wolfbeis; *Methods. Appl. Fluoresc.*, **2021**, *9*, 042001.
67. M. Rahman; Z. Muhseen; M. Junaid; H. Zhang; *Curr. Protein. Pept. Sci.*, **2015**, *16*, 502-512.
68. D.A. Dougherty; *Science*, **1996**, *271*, 163-168.
69. F. Neese; Software update: The ORCA program system—Version 5.0, *WIREs Comp. Mol. Sci.*, **2022**, 12.
70. A.D. Becke; *J. Chem. Phys.*, **1993**, *98*,1372-1377.
71. C. Lee; W. Yang; R.G. Parr; *Phys. Rev. B.*, **1988**, *37*, 785-789.
72. S.H. Vosko; L. Wilk; M. Nusair, *Can. J. Phys.*, **1980**, *58*, 1200-1211.
73. P.J. Stephens; F.J. Devlin; C.F. Chabalowski; M.J. Frisch; *J. Phys Chem.*, **1994**, *98*, 11623-11627.
74. S. Grimme; J. Antony; S. Ehrlich; H. Krieg; *J. Chem. Phys.*, **2010**, *132*, 154104.
75. S. Grimme; S. Ehrlich; L. Goerigk; *J. Comput. Chem.* **2011**, *32*, 1456-1465.
76. F. Weigend; R. Ahlrichs; *Phy. Chem.*, **2005**, *7*, 3297.
77. H. R. Christofk; M. G. V. Heiden; N. Wu; J. M. Asara; L. C. Cantley; *Nature*, **2008**, *452*, 181-186.
78. H. Lineweaver; D. Burk; *J. Am. Chem. Soc.*, **1934**, *56*, 658-666.
79. N. M. O'Boyle; M. Banck; C.A. James; C. Morley; T. Vandermeersch; G. R. Hutchison; *J. Cheminform.*, **2011**, *3*, 33.
80. T.M. Larsen; L.T. Laughlin; H.M. Holden; I. Rayment; G.H. Reed; *Biochemistry*, **1994**, *33*: 6301-6309
81. Dassault Systèmes BIOVIA, **2020** Discovery studio 2020 Client.
82. A. Daina; O. Michielin; V. Zoete; *Sci. Rep.*, **2017**, *7*, 42717.
83. M. Lobell; M. Hendrix; B. Hinzen; J. Keldenich; H. Meier; C. Schreck; R. Schohe-Loop; T. Wunberg; A. Hillisch; *ChemMedChem.* **2006**, *1*, 1229-1236.
84. A. Daina; O. Michielin; V. Zoete; *J. Chem. Inf. Model.* **2014**, *54*, 3284-3

